Accepted Manuscript

Title: TiO_2 nanotubes grown on Ti substrates with different microstructure

Authors: Hanna Sopha, Karel Tesar, Petr Knotek, Ales Jäger, Ludek Hromadko, Jan M. Macak

PII: S0025-5408(17)34696-2
DOI: https://doi.org/10.1016/j.materresbull.2018.03.036
Reference: MRB 9917

To appear in: *MRB*

Received date: 21-12-2017
Revised date: 14-3-2018
Accepted date: 19-3-2018

Please cite this article as: Sopha H, Tesar K, Knotek P, Jäger A, Hromadko L, Macak JM, TiO_2 nanotubes grown on Ti substrates with different microstructure, *Materials Research Bulletin* (2010), https://doi.org/10.1016/j.materresbull.2018.03.036

TiO_2 nanotubes grown on Ti substrates with different microstructure

Hanna Sopha[a], Karel Tesar[b,c], Petr Knotek[d], Ales Jäger[e], Ludek Hromadko[a], Jan M. Macak[a,f,*]

[a]*Center of Materials and Nanotechnologies, Faculty of Chemical Technology, University of Pardubice, Nam. Cs. Legii 565, 53002 Pardubice, Czech Republic*

[b]*Department of Dieletrics, Institute of Physics of the Czech Academy of Sciences, Na Slovance 2, 182 21 Prague 8, Czech Republic*

[c]*Department of Materials, Faculty of Nuclear Sciences and Physical Engineering, Czech Technical University, Trojanova 13, 120 00 Prague 2, Czech Republic*

[d]*Department of General and Inorganic Chemistry, Faculty of Chemical Technology, University of Pardubice, Studentska 573, 532 10 Pardubice, Czech Republic*

[e]*Department of Mechanics, Faculty of Civil Engineering, Czech Technical University in Prague, Thákurova 7, 16629 Prague 6, Czech Republic*

[f] *Central European Institute of Technology, Brno University of Technology, Purkynova 123, 61200 Brno, Czech Republic*

**Corresponding Author: e-mail: jan.macak@upce.cz*

Phone: +420-466 037 401

GRAPHICAL ABSTRACT

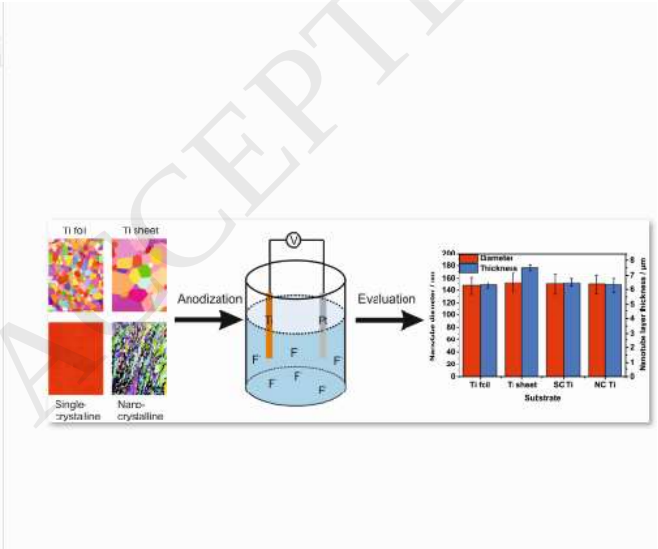

HIGHLIGHT

- TiO_2 nanotube layers were grown on four different Ti substrates by anodization
- Ti substrates with completely different microstructures were used
- The grain size of the substrates ranged from nanocrystalline to single-crystalline
- Differences between the nanotubes grown on these substrates were evaluated
- Similar nanotube dimensions were received on all Ti substrates

Abstract

Four Ti substrates with various microstructures were investigated for the anodic growth of TiO_2 nanotube layers: nanocrystalline and single-crystalline ingots as well as microcrystalline thick Ti sheets and microcrystalline thin Ti foils. All substrates were anodized in a conventional ethylene glycol based electrolyte under identical conditions. The resulting TiO_2 nanotube layers were compared in dimensions and the consumption of Ti required for their growth. Unexpectedly, the results showed that on all substrates nanotube layers with a similar thickness and nanotube diameter, as well as a similar degree of ordering and after annealing the same crystallographic orientation of anatase were received, regardless the microstructures. However, the nanotube layers grown on a Ti sheet revealed a slightly higher thickness compared to the other substrates which were assigned to slower field-assisted dissolution rates due to different impurities found in this substrate compared to other ones.

Keywords: titanium, titanium dioxide, nanotubes, anodic oxidation, microstructure

Introduction

Since their first introduction in 1984 [1], TiO_2 nanotube layers have attracted great interests due to their wide applications in various fields, as described extensively in several reviews [2-4]. During the recent years, significant knowledge has been gained about the influence of the anodization conditions on the growth and properties of TiO_2 nanotube layers [5-7]. In addition, efforts were carried out to prepare hexagonally ordered TiO_2 nanotube layers [8-15] resulting in perfectly organized nanotubes shown recently [13-15], with similarly perfect ordering as the nanoporous Al_2O_3 [16,17].

Titanium is a valve metal typically having a hexagonal close packed structure (α-Ti) consisting of grains with different crystallographic orientations and sizes [18]. Ti substrates exist with

various microstructures and chemical grades, depending on the processing route [19]. The physical, chemical and electrochemical properties of these Ti substrates are influenced by the crystallographic defects and impurities the Ti [20,21], as any other solid substance, contains.

It can be expected that the microstructure of the crystalline Ti substrates has to play an important role for the growth of the TiO_2 nanotube layers. Several reports on the influence of the microstructure of the substrate on the TiO_2 nanotube growth have already been published to address this expectation. It was shown that in some aqueous electrolytes some grain orientations are nanotube retarding [22] or that non-uniform nanotube layers were received due to the grain structure [23,24]. However, recently we showed that in ethylene glycol based electrolytes, no grain orientation was nanotube growth retarding, but a sufficient anodization time was required to obtain TiO_2 nanotube layers without the remnant porous initial oxide [25]. The microstructure of the Ti substrates does not exclusively influence the nanotube growth (i.e. whether and how the tube layers will grow), but might also influence the resulting ordering of the nanotube layers. As shown recently, locally highly ordered TiO_2 nanotube layers were observed on the different grains but, in the vicinity of the grain boundaries, the order was disturbed [19]. Su et al. [26] showed that on polycrystalline Ti foils a bimodal pore size distribution was received on different grains, while monomodally distributed TiO_2 nanotube layers were achieved upon anodization of (0001) oriented Ti films sputtered on conductive glass. Therefore, the use of nanocrystalline or, opposite, single-crystalline Ti substrates can be interesting for the growth of highly ordered nanotube layers.

Zhang and Han refined the grain size of Ti substrates by surface mechanical attrition treatment [27]. Upon anodization of these Ti substrates with nanocrystalline structure in a glycol (not further specified) based electrolyte, the authors obtained a thicker TiO_2 nanotube layer compared to the as-received commercial Ti substrates. They ascribed the differences in the TiO_2 nanotube layer thickness to an accelerated growth rate due to an increased density of grain boundaries and dislocations in the nanocrystalline substrates. Ferreira et al. annealed Ti substrates at 1000 °C before anodization to reduce crystalline defects and increase the grain size [28]. However, the authors received more uniform and thicker nanotube layers on the non-modified Ti substrates after anodization in HF containing aqueous solution. Finally, Hu et al. produced Ti substrates with grain sizes between 140 nm and 35 µm using high pressure torsion [29]. After two-step anodization in a glycerol based electrolyte slightly thicker nanotube layers with a less pronounced scatter in nanotube diameter were obtained on Ti substrates with smaller grain sizes. However, in another study [30] the same authors showed that, using a glycerol

based electrolyte of the same nominal composition, the microstructure of the Ti substrate did not have a significant influence on the nanotube diameter after one-step anodization.

All these reports clearly show that there is some influence of the microstructure on the nanotube layer growth, in particular on the nanotube dimensions. However, exact reasons remain somewhat ambiguous and are by far not very clear. Additionally, no study compared single-crystalline Ti ingots or foils, with nanocrystalline and microcrystalline substrates for anodization under identical conditions in terms of the TiO_2 nanotube dimensions and ordering. Thus, in this work, for the first time, the growth and the order of nanotube layers on conventional Ti sheets and thin foils was compared with nanocrystalline and single-crystalline Ti substrates under otherwise identical conditions. A range of characterization methods was applied to investigate the influence of microstructures on the nanotube growth and ordering.

Experimental

Four different Ti substrates were used, namely polycrystalline Ti sheets (Goodfellow, 2 mm, 99.6+% purity), Ti foils (Sigma-Aldrich, 0.127 mm, 99.7% purity), single-crystalline Ti (MaTeck, 99.99% purity, polished to a roughness R_{RMS} (root mean square) < 10 nm before delivery) and nanocrystalline Ti prepared via equal channel angular pressing with applied back pressure (ECAP-BP). The processing conditions of the latter substrate were described previously [31]. Before the anodization the nanocrystalline Ti was carefully grinded on an emery paper (P1200) to remove an eroded layer left on the samples the after electrical discharge machining. The other Ti substrates were used as received.

The four different substrates were anodized at 60 V for 4 h in an ethylene glycol based electrolyte containing 10 vol. % H_2O and 150 mM NH_4F. To receive electrolytes of the same composition and age [32], the base electrolyte was split into four equal parts after aging and each part was used for the anodization of one Ti substrate. The electrochemical cell consisted of a 2 electrode configuration using a Pt foil as the counter electrode, while the Ti substrates (working electrodes) were pressed against an O-ring of the electrochemical cell, leaving 0.071 cm^2 open to an electrolyte. Electrochemical experiments were carried out at room temperature employing a high-voltage potentiostat (PGU–200 V, IPS Elektroniklabor GmbH). All experiments were carried out twice for each substrate. After anodization the Ti substrates were rinsed and sonicated in isopropanol and dried in air.

The structure and morphology of the TiO_2 nanotube layers were characterized by a field-emission scanning electron microscope (SEM, JEOL JSM 7500F). The dimensions (diameter

and length) of the nanotube layers were measured and statistically evaluated using proprietary Nanomeasure software.

To obtain an adequate surface for Electron Backscatter Diffraction (EBSD) the substrates were grinded using P2400 SiC paper and then electrolytically polished using Struers LectroPol-5 with A3 electrolyte, at 253 K, 20V for 30 s. The microstructural analyses of the different crystalline Ti substrates were carried out by EBSD technique using a Microprobe JEOL 733 or Dual Beam FEI Quanta 3D FEG; both fitted with an EDAX EBSD detector. EBSD data was analysed with TSL OIM software to obtain inverse pole figures (IPF), IPF maps and the grain size distribution. The grain tolerance angle for the recognition of neighbouring grains was set to 5°.

The chemical composition of the substrates was determined by glow-discharge optical emission spectroscopy (GD-OES, Spectruma GDA 750HR). A direct current method with a voltage of 1000 V, a current 20 mA and a chamber pressure of ~2.4 hPa was utilized for the measurements. Certified reference materials were used for the measurement calibration.

Atomic Force Microscopy (AFM, Solver Pro M, NT-MDT) measurements were carried out to evaluate the surface topography of the substrates in semi-contact mode following the anodization, on the area of 5 x 5 μm^2, according to conditions described in [33]. The roughness of the Ti non-treated samples (in form of the root mean square – RMS) was calculated from the topology determined by a digital holographic microscope (DHM, R1000, Lyncée Tec) from at least three individual measurements from the profiles with the length over 300 µm [34]. The depth profiles of the craters left on the substrates after removing the nanotube layers after the anodization were measured using a mechanical profilometer (SSC-01, RMI Ltd.) [19].

Before X-ray diffraction (XRD) measurements, all nanotube layers were annealed at 400 °C for 1 hour (heating rate: 2.1 °C/min). Microdiffraction analyses were carried out using 3 kW diffractometer Smartlab from Rigaku equipped by detector Dtex Ultra. The diffractometer was set up in parallel beam geometry, additionally focused by a collimator to a beam spot of size 0.5mm. The Cu lamp operated at current 30 mA and voltage 40 kV.

Results and discussion

Figure 1 shows the inverse pole figure maps, the inverse pole figures (IPF) and the direct pole figures of all Ti substrates investigated in this study, namely a thin Ti foil, a thick Ti sheet, a single-crystalline Ti substrate and a nanocrystalline Ti substrate. As expected, all substrates,

except the single-crystalline one, were polycrystalline with different grain sizes. In case of the polycrystalline substrates, the largest grains were found for the sheet with an average grain size of 25 ± 16 µm, followed by the foil with an average grain size of 8 ± 5 µm. The nanocrystalline substrate had at some parts a grain size of 100 - 200 nm, however other parts of the substrate showed unrecrystallized regions i.e. highly deformed regions with a very high concentration of defects. In the black regions of the IPF map of for the nanocrystalline Ti, EBSD was not able to acquire any signal due to a high defect concentration. Thus, no information could be extracted about grains.

The inverse pole figures (IPF) show that the texture (i.e. the statistical representation of crystallographic orientations) was different for the four substrates. The orientation of the single-crystalline substrate was solely (0001), in line with the manufacturer´s specification. In case of the Ti sheet and the Ti foil, most of the grains were also oriented towards the (0001) direction. However, for the nanocrystalline substrate less grains with a (0001) orientation were found and c-axes of the grains were rather aligned perpendicular to the surface. The texture plots, represented by direct pole figures, also shown in Fig.1, clearly confirm this observation. As shown by Jager et al. [31], the resulting texture of the nanocrystalline sample obtained by EBSD is after proper rotation of the sample reference frame almost identical to the texture measured by x-ray diffraction.

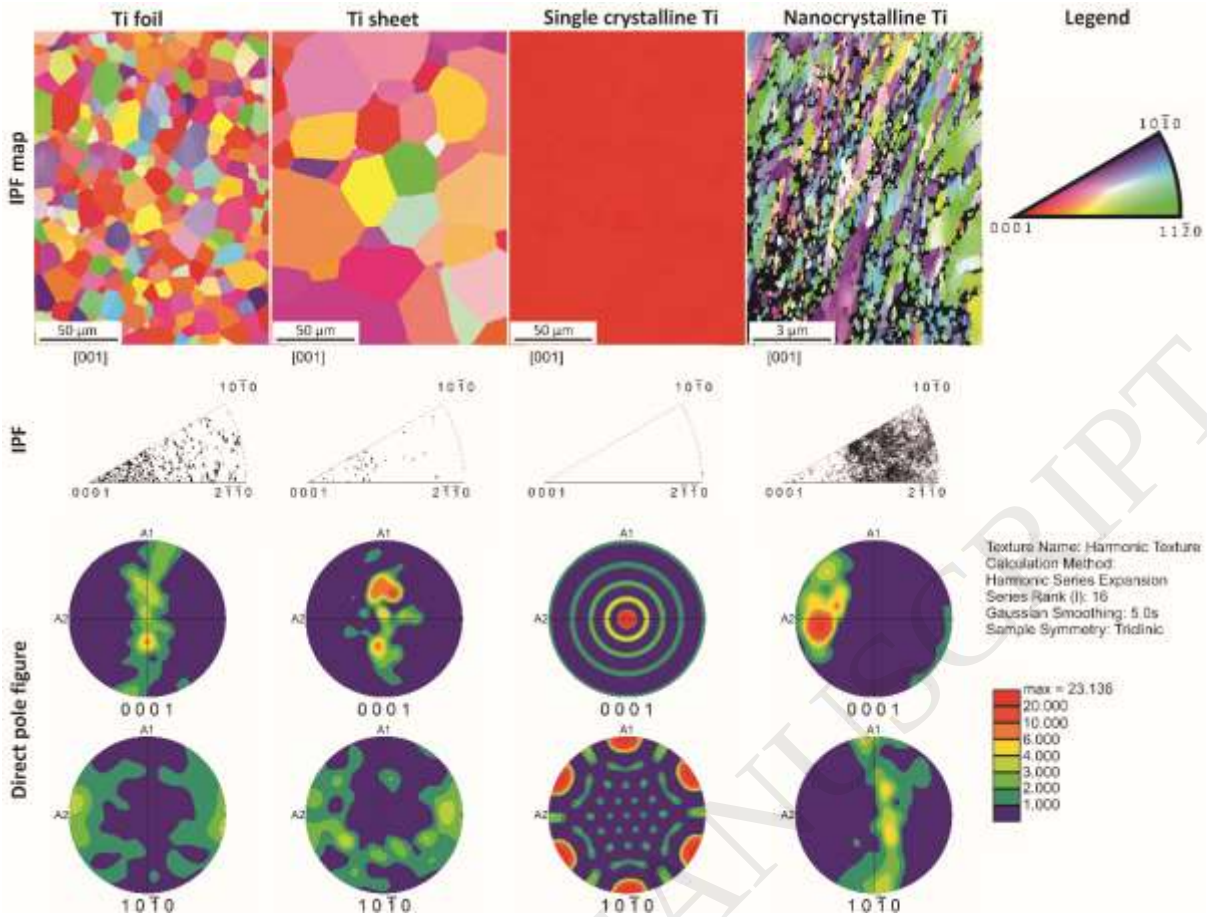

Figure 1. EBSD analyses of the substrates: inverse pole figure maps (IPF map), inverse pole figures (IPF) and direct pole figures of the Ti foil, Ti sheet, single-crystalline Ti and nanocrystalline Ti. Note different scale bar in IPF map for the nanocrystalline Ti.

It has to be pointed out that for the anodizations one base electrolyte was prepared and split into four equivalent portions to have equal electrolytes, i.e. electrolytes of the same composition and age, for the anodizations of the different substrates. This is especially important since small differences in the composition of ethylene glycol based electrolytes can lead to differences in the current-time plots and in the nanotube dimensions [32].

The polarization plots and current transients for the four different Ti substrates upon anodization at 60 V in an ethylene glycol based electrolyte are shown in Figure 2. It can be seen, that all substrates exhibited similar curves which resemble the typical anodization behaviour of Ti with three distinct stages. This behaviour has been extensively described in the literature [2, 35]. However, differences in the polarization curves and current density transients can be seen in the absolute current density values measured at the beginning of the anodizations of the four different Ti substrates. It is known from the literature [19,36] that higher initial

current densities are obtained when the Ti substrates have a higher roughness. Thus, the differences in the current densities which can be seen in the polarization curves in Fig. 2 can be connected with the different initial roughness of the substrates (see Table 1). The roughness of the single-crystalline substrate was not measured. However, the substrate was polished by the producer to a roughness R_{RMS} < 10 nm. Thus, the single-crystalline substrate had the lowest roughness, which is in agreement with the lowest absolute initial current density.

More important for the present study is the steady state current density at the end of the anodization, where the layer growth is terminated and the nanotube dimensions are compared (see inset in Figure 2). After four hours of anodization, similar steady state current densities were recorded for all Ti substrates, ranging between ~0.45 and ~0.55 mA cm^{-2}. In the literature, the difference in current densities during the anodization of different substrates is often assigned to stress on the Ti substrates´ surface due to grain boundaries [19]. Nevertheless, in the case of the single-crystalline substrate, no grain boundaries were observed, as shown in Fig. 1, but still no significant variations among the substrates were obtained in the current densities. Thus, grain boundaries are not exclusively responsible for this behaviour and other influences must also be taken into account.

Another factor that can affect the current densities, is the content of impurities in the Ti substrates, as already shown in our previous work on substrates obtained from different producers [19]. In this work, GD-OES measurements were carried out for all four Ti substrates employed herein. The five main impurities for each substrate are listed in Table 2. As can be seen, for all Ti substrates, except the Ti sheet, Fe and V were the main impurities. Similar to the other substrates, the Ti sheet contained Fe as the main impurity but the second impurity was Al. This is interesting since Al does not readily dissolve during anodization, but it passivates the Ti surface [37,38], while V, present in the other substrates in higher amount, hardly forms an oxide in the used electrolyte and mainly dissolves [19]. This is in agreement with the measured crater depth, i.e. the average height difference between the non-anodized and the anodized area of the Ti substrates after removal of the nanotube layers, given in Table 1: while the Ti foil and the nanocrystalline substrate (V richer) showed similar crater depth of ~2.5 µm, the crater on the Ti sheet (Al richer) was shallower (~1.4 µm). Unfortunately, the crater depth on the single-crystalline substrate could not be measured after destructive GD-OES measurements. It must be stated that the impurities of the Ti substrates are not embedded into the TiO_2 nanotubes, as a recent study shows [39].

The Coulombic growth efficiencies (represented by a ratio of the charge devoted to the nanotube growth and the total charge passed through the electrochemical cell) were calculated

in order to assess the effectiveness of the consumption of the Ti during anodization for the nanotube growth, as described previously in [40]. The calculations considered porosity of nanotube layers of approx. 20 % and yielded efficiencies of 27.3 %, 27.1 %, 21.5 % and 19.3 % for the anodization of the single-crystalline substrate, the Ti thick sheet, the Ti thin foil and the nanocrystalline substrate. This in accordance with the measured crater depth - a lower current efficiency results in a deeper crater due to stronger dissolution of the TiO_2 being formed upon anodization.

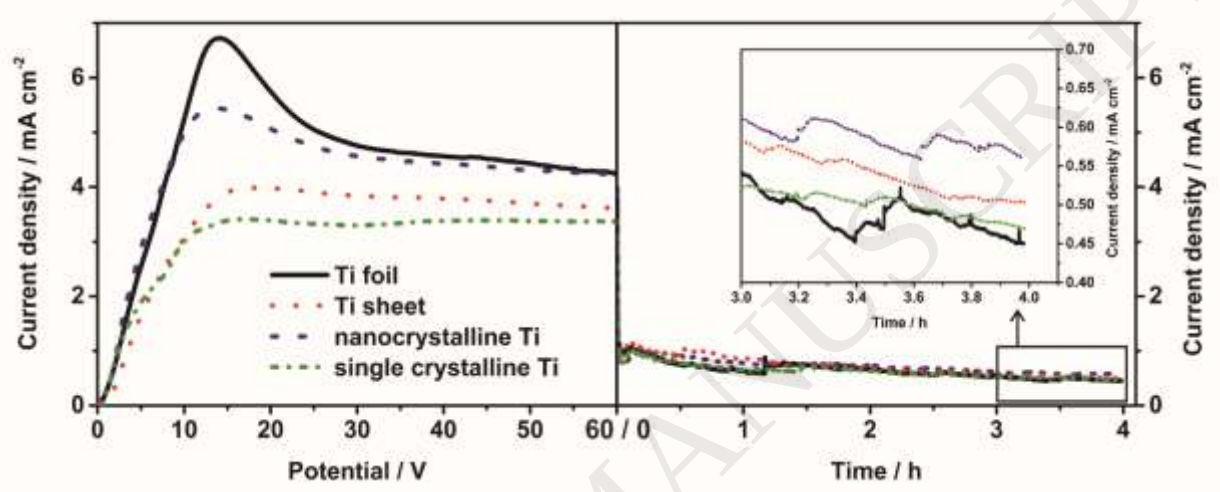

Figure 2. Polarization plots (left) and current density transients (right) recorded during the anodization at 60 V for 4 h for four different Ti substrates.

Table 1: Roughness of the initial Ti substrates (acquired by DHM), and depth difference between the non-anodized area and the anodized area of the Ti substrate (acquired by profilometer). NC Ti – nanocrystalline Ti, SC – Single-crystalline Ti.

Substrate	RMS of the Ti roughness (nm)	Average crater depth (µm)
Ti foil	100.2	2.45
Ti sheet	52.4	1.56
NC Ti	53.0	2.56
SC Ti	< 10	n/a

Table 2: Average Ti content and the average content of the five main impurities of the Ti substrates measured by GD-OES, given in weight %. SC – Single-crystalline Ti, NC Ti – nanocrystalline Ti.

Substrate	Ti	Impurity 1	Impurity 2	Impurity 3	Impurity 4	Impurity 5

Ti foil	99.91	Fe – 0.055	V – 0.040	Cu – 0.016	Cr – 0.015	Si – 0.005
Ti sheet	99.94	Fe – 0.038	Al – 0.021	V – 0.015	Cu – 0.008	Cr – 0.006
NC Ti	99.88	V – 0.045	Fe – 0.035	Cu – 0.028	Al – 0.009	Si – 0.007
SC Ti	99.92	Fe – 0.057	V – 0.026	Si – 0.015	Al – 0.013	Cu – 0.009

Figure 3 shows top views and cross-sectional SEM images of the nanotube layers grown on the different substrates. Obviously, on all used substrates uniform nanotube layers were received over the whole anodized area, which grew very straight and were free of grass or remnant porous oxide. In particular, this is also the case for the nanocrystalline substrate. This has to be pointed out since this substrate showed some unrecrystallized, highly deformed regions with a very high concentration of defects, as described above. That means that the unrecrystallized, deformed regions of the Ti substrate did not influence the TiO_2 nanotube growth.

Figure 4 summarizes the average inner nanotube diameters and nanotube layer thicknesses measured for the four different substrates. Interestingly, hardly any differences in the average diameter (measured on nanotubes distributed over the whole nanotube layer) were observed among the resulting values: 147.4 ± 14.2 nm, 152.9 ± 15.3 nm, 149.6 ± 15.6 nm and 149.9 ± 16.5 nm for nanotube layers grown on the Ti foil, the Ti sheet, the single-crystalline Ti substrate and the nanocrystalline Ti substrate, respectively. Similarly, no differences were found for the nanotube layer thickness on the Ti foil, the single-crystalline Ti and at the nanocrystalline Ti substrate with average thicknesses of 6.3 ± 0.2 µm, 6.5 ± 0.3 µm and 6.3 ± 0.5 µm, respectively. However, thicker nanotube layers were received on the Ti sheet with an average thickness of 7.5 ± 0.2 µm. This is interesting, since, as described earlier, the shallowest crater was obtained on this substrate (after removal of the nanotube layer). This might be due to the relatively high Al content in the Ti sheet, as revealed by GD-OES. The thickness of the nanotube layers was in all cases higher than the depth of the crater after the nanotube removal. This is due to the volume expansion during the oxide formation and in accordance with the literature [41].

Hu et al. [29] showed that on Ti substrates with a fine grained microstructure, slightly thicker nanotube layers than on Ti substrates with coarse grains can be received upon two-step anodization in glycerol based electrolyte with a low water content, due to increased stresses and more defects in the Ti substrates with smaller grains. However, the same authors showed in another study [30] that the microstructure of the Ti substrates does not have an influence on the bottom diameter of the nanotubes prepared in the same electrolyte after one-step anodization. Our previous work [19] showed that nanotube layers with different average

diameters and length were obtained upon the anodization of Ti foil of various producers in ethylene glycol based electrolytes with a low water content.

The reasons for the opposite observation in this study remain still unclear. Nevertheless, this study shows that the microstructure of the substrates does not necessarily influence the nanotube dimensions. One could assume that the situation is of higher complexity and that there is an interplay between several different factors, which are important for the nanotube dimensions. These factors include the specific anodization conditions, the selection of Ti substrates (microstructure, impurities), the choice of the electrolyte (e.g. in this study an ethylene glycol based electrolyte with a relatively high water content compared to the other mentioned studies was used), the temperature, etc.

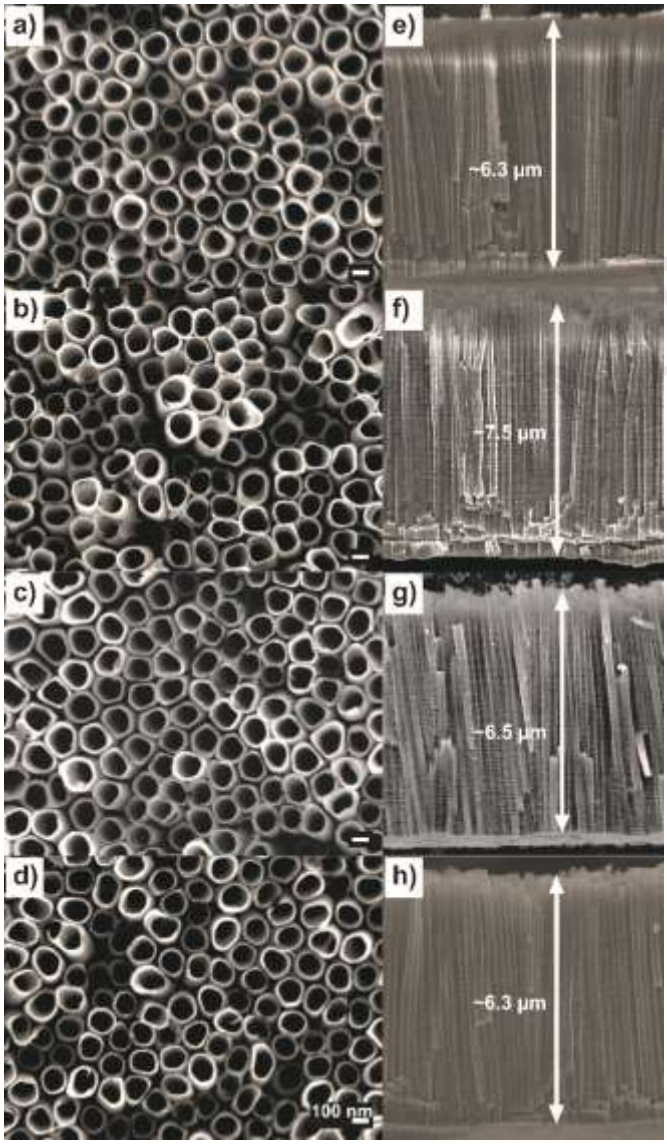

Figure 3. SEM top views (left column) and cross section views (right column) of the TiO_2 nanotube layers on Ti foil (a,e), the Ti sheet (b,f), the single-crystalline Ti (c,g), and the

nanocrystalline substrate (d,h). All bars in the left column show 100 nm. The arrows in the right column indicate the average thickness of the nanotube layers grown on the different substrates.

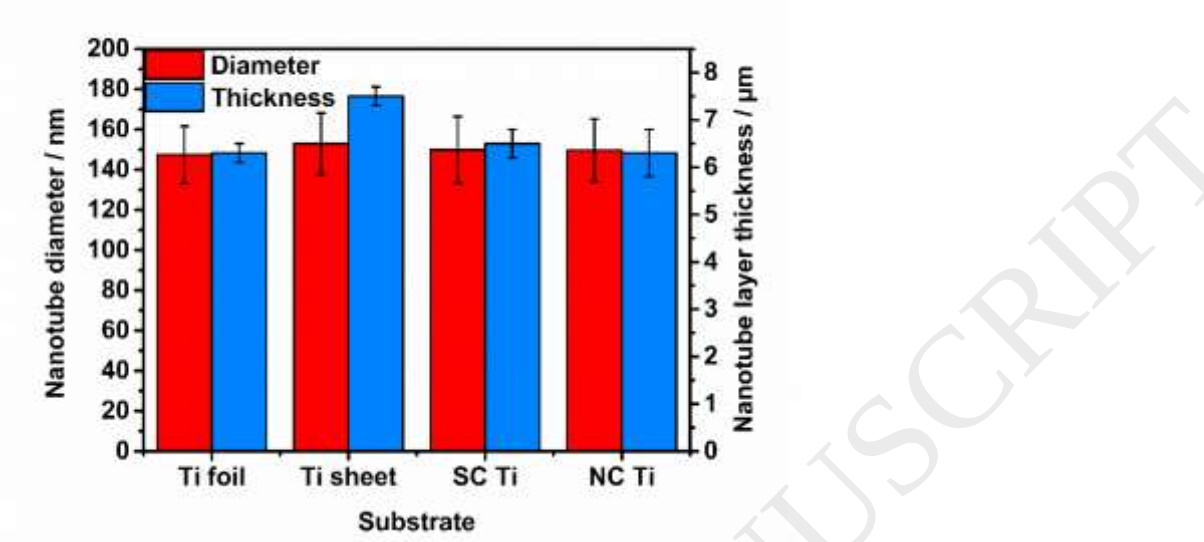

Figure 4. Evaluation of the average inner diameter and the average thickness of the nanotube layers grown on the different substrates at 60 V for 4 h.

AFM investigations were carried out on the anodized area of the Ti substrate after the removal of the TiO_2 nanotube layers. Figure 5 shows AFM images of the dimples imprinted on the Ti substrates after removal of the TiO_2 nanotube layers. These dimples resemble the structure of the previous nanotube layer [8,42]. As can be seen, no significant differences could be observed between the different substrates. All substrates showed some variation in the diameter of the dimples, as well as in the dimple depth and the local ordering. Usually, these local differences are explained with the grain microstructure of the substrates, concluding that nanotubes grow slightly differently on grains with different orientations. [19,26]. However, these differences in the nanotube diameter and in the dimple depth were found on all substrates including the single-crystalline substrate. Furthermore, in the case of the nanocrystalline Ti substrate, it must be noted that the average nanotube diameter was of approximately the same size as the Ti grains of the substrate, which were in the recrystallized areas between 100 and 200 nm in diameter as described above. Thus, it can be concluded that the grain structure of the Ti substrates with local stress at the grain boundaries is not the (only) reason for the local ordering of the nanotube layers. Instead, the differences must also be connected to other factors, for instance different field-assisted dissolution rates due to local variations in the concentration of the impurities.

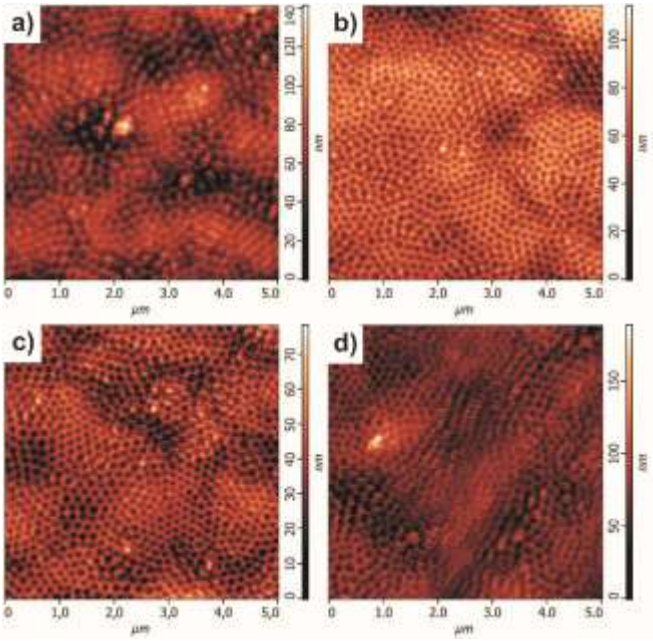

Figure 5. AFM images of dimples imprinted in the Ti substrates after the nanotube layer removal from a) the Ti foil, b) the Ti sheet, c) the single-crystalline Ti, and d) the nanocrystalline substrate.

Finally, XRD characterizations of the TiO_2 nanotube layers were carried out after annealing at 400 °C to convert the as-anodized nanotube layers from amorphous into anatase phase. The XRD patterns are shown in Figure 6. No significant differences in the crystallographic planes of anatase between the four different Ti substrates can be seen. In all cases the (101) peak was the main anatase peak. Furthermore, signals for anatase (200), (105), (211), and (204) were received with (200) showing the second highest intensity. Just in case of the nanocrystalline substrate the signal at $2\theta \approx 63$ deg (corresponding to the anatase (204) plane) was more pronounced than for the other three Ti substrates. However, in this region two signals are very close to each other: the anatase (204) signal ($2\theta = 62.750$ deg) and the Ti (110) signal ($2\theta = 62.965$ deg). Thus, the high intensity of this signal might be due to an overlay of the two signals here.

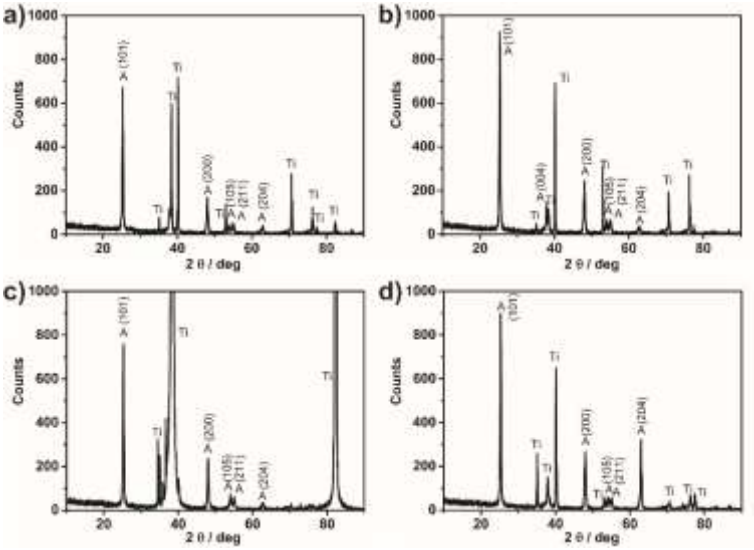

Figure 5. XRD patterns of the TiO_2 nanotube layers on a) Ti foil, b) Ti sheet, c) single-crystalline Ti, and d) nanocrystalline Ti after annealing at 400 °C with indicated crystallographic planes for anatase. A – anatase, Ti – titanium.

Conclusions

In summary, the present work demonstrates that TiO_2 nanotube layers with similar dimensions, namely diameter and thickness, can be received upon identical anodization procedure of Ti substrates, beside totally different microstructure. Furthermore, after annealing at 400 °C all TiO_2 nanotube layers show the same crystallographic planes. Thus, the microstructure of the Ti substrates may not necessarily have a dominant influence on the nanotube dimensions as one could assume and as envisaged in previous studies. This suggests that there are other significant factors influencing the nanotube growth and the resulting nanotube dimensions, such as chemical impurities, as well as the choice of the anodization electrolyte. More efforts need to be carried out to understand these factors in more detail.

Acknowledgements

The European Research Council (project nr. 638857) and the Ministry of Youth Education and Sports of the Czech Republic (projects nr. LM2015082, 8F15004, LQ1601) are acknowledged for financial support of this work. Financial support of the Czech Technical University in Prague in the frame of the project SGS16/249/OHK4/3T/14 is also gratefully acknowledged.

References

[1] M. Assefpour-Dezfuly, C. Vlachos, E. H. Andrews, Oxide morphology and adhesive bonding on titanium surfaces, J. Mater. Sci. 19 (1984) 3626-3639.

[2] J.M. Macak, H. Tsuchiya, A. Ghicov, K. Yasuda, R. Hahn, S. Bauer, P. Schmuki, TiO_2 nanotubes: Self-organized electrochemical formation, properties and applications, Curr. Opin. Solid State Mat. Sci. 11 (2007) 3-18.

[3] D. Kowalski, D. Kim, P. Schmuki, TiO_2 nanotubes, nanochannels and mesosponge: Self-organized formation and applications, Nano Today 8 (2013) 235-264.

[4] K. Lee, A. Mazare, P. Schmuki, One-dimensional titanium dioxide nanomaterials: nanotubes, Chem. Rev. 114 (2014) 9385-9454.

[5] S. Bauer, S. Kleber, P. Schmuki, TiO_2 nanotubes: Tailoring the geometry in H_3PO_4/HF electrolytes, Electrochem. Commun. 8 (2006) 1321–1325.

[6] J.M. Macak, H. Hildebrand, U. Marten-Jahns, P. Schmuki, Mechanistic aspects and growth of large diameter self-organized TiO_2 nanotubes, Journal of Electroanal. Chem. 621 (2008) 254–266.

[7] A. Ghicov, H. Tsuchiya, J. M. Macak, P. Schmuki, Titanium oxide nanotubes prepared in phosphate electrolytes, Electrochem. Commun. 7 (2005) 505–509.

[8] J.M. Macak, S.P. Albu, P. Schmuki, Towards ideal self-ordering of TiO_2 nanotubes, Phys. Stat. Sol. (RRL) 1 (2007) 181-183.

[9] G. Zhang, H. Huang, Y. Zhang, H.L.W. Chan, L. Zhou, Highly ordered nanoporous TiO_2 and its photocatalytic properties, Electrochem. Commun. 9 (2007) 2854-2858.

[10] S. Li, G. Zhang, D. Guo, L. Yu, Wei Zhang, Anodization fabrication of highly ordered TiO_2 nanotubes, J. Phys. Chem. C 113 (2009) 12759-12765.

[11] J. Choi, R.B. Wehrspohn, J. Lee, U. Gösele, Anodization of nanoimprinted titanium: a comparison with formation of porous alumina, Electrochim. Acta 49 (2004) 2645-2652.

[12] B. Chen, K. Lu, Z. Tian, Effects of titania nanotube distance and arrangement during focused ion beam guided anodization, J. Mater. Chem. 21 (2011) 8835-8840.

[13] T. Kondo, S. Nagao, T. Yanagishita, N.T. Nguyen, K. Lee, P. Schmuki, H. Masuda, Ideally ordered porous TiO_2 prepared by anodization of pretextured Ti by nanoimprinting process, Electrochem. Commun. 50 (2015) 73-76.

[14] V. Vega, J.M. Montero-Moreno, J. Garcia, V.M. Prida, W. Rahimi, M. Waleczek, C. Bae, R. Zierold, K. Nielsch, Long-range hexagonal arrangement of TiO_2 nanotubes by soft lithography-guided anodization, Electrochim. Acta 203 (2016) 51-58.

[15] H. Sopha, T. Samoril, E. Palesch, L. Hromadko, R. Zazpe, D. Skoda, M. Urbanek, S. Ng, J. Prikryl, J.M. Macak, Ideally hexagonally ordered TiO_2 nanotube arrays, Chemistry Open 6 (2017) 480-483.

[16] H. Masuda, K. Fukuda, Ordered metal nanohole arrays made by a two-step replication of honeycomb structures of anodic alumina, Science, 268 (1995) 1466-1468.

[17] H. Masuda, H. Yamada, M. Satoh, H. Asoh, M. Nakao, and T. Tamamura, Highly ordered nanochannel-array architecture in anodic alumina, Appl. Phys. Lett., 71 (1997) 2770-2772.

[18] M.J. Donachie, Titanium: A Technical Guide, 2nd ed., ASM International, 2007.

[19] H. Sopha, A. Jäger, P. Knotek, K. Tesar, M. Jarosova, J.M. Macak, Self-organized anodic TiO_2 nanotube layers: Influence of the Ti substrate on nanotube growth and dimensions, Electrochim. Acta 190 (2016) 744-752.

[20] Lu, Z. Tian, J. A. Geldmeier, Polishing effect on anodic titania nanotube formation, Electrochim. Acta 56 (2011) 6014–6020.

[21] U. König, B. Davepon, Microstructure of polycrystalline Ti and its microelectrochemical properties by means of electron-backscattering diffraction (EBSD), Electrochim. Acta 47 (2001) 149-160.

[22] A. Crawford, N. Chawla, Tailoring TiO_2 nanotube growth during anodic oxidation by crystallographic orientation of Ti, Scripta Mater. 60 (2009) 874–877.

[23] S. Leonardi, A.l. Bassi, V. Russo, F. Di Fonzo, O. Paschos, T. M. Murray, H. Efstathiadis, J. Kunze, TiO_2 nanotubes: Interdependence of substrate grain orientation and growth characteristics, J. Phys. Chem. C 116 (2012) 384–392.

[24] S. Leonardi, V. Russo, A. L. Bassi, F. Di Fonzo, T. M. Murray, H. Efstathiadis, A. Agnoli, J. Kunze-Liebhäuser, TiO_2 nanotubes: Interdependence of substrate grain orientation and growth rate, ACS Appl. Mater. Interfaces 7 (2015) 1662–1668.

[25] J.M. Macak, M. Jarosova, A. Jäger, H. Sopha, M. Klementova, Influence of the Ti microstructure on anodic self-organized TiO_2 nanotube layers produced in ethylene glycol electrolytes, Appl. Surf. Sci. 371 (2016) 607-612.

[26] Z. Su, L. Zhang, F. Jiang, W. Zhou, Z. Deng, Y. Cao, M. Hong, Formation of anodic TiO_2 nanotube arrays with bimodal pore size distribution, Electrochem. Commun. 31 (2013) 67-70.

[27] L. Zhang, Y. Han, Effect of nanostructured titanium on anodization growth of self-organized TiO_2 nanotubes, Nanotechnology 21 (2010) 055602 (8pp).

[28] C.P. Ferreira, M.C. Goncalves, R. Caram, R. Bertazzoli, C.A. Rodrigues, Effects of substrate microstructure on the formation of oriented oxide nanotube arrays on Ti and Ti alloys, Appl. Surf. Sci. 285P (2013) 226-234.

[29] N. Hu, N, Gao, Y. Chen, M.J. Starink, Achieving homogeneous anodic TiO_2 nanotube layers through grain refinement of the titanium substrate, Mater. Des. 110 (2016) 346-353.

[30] N. Hu, N. Gao, M. J. Starink, The influence of surface roughness and high pressure torsion on the growth of anodic titania nanotubes on pure titanium, Appl. Surf. Sci. 387 (2016) 1010–1020.

[31] A. Jäger, V. Gärtnerova, K. Tesař, Microstructure and anisotropy of the mechanical properties in commercially pure titanium after equal channel angular pressing with back pressure at room temperature, Mater. Sci. Eng. A 644 (2015) 114-120.

[32] H. Sopha, L. Hromadko, K. Nechvilova, J.M. Macak, Effect of the electrolyte age and potential changes on the morphology of TiO_2 nanotubes, J. Electroanal. Chem. 759 (2015) 122-128.

[33] P. Knotek, E. Chanova, F. Rypacek, AFM imaging and analysis of local mechanical properties for detection of surface pattern of functional groups, Mater. Sci. Eng., C 33 (2013) 1963.

[34] P. Knotek, D. Arsova, E. Vateva, L. Tichy, Photo-expansion in Ge-As-S amorphous film monitored by digital holographic microscopy and atomic force microscopy, J. Optoelectron. Adv. Mater 11 (2009) 391.

[35] K. Yasuda, J.M. Macak, S. Berger, A. Ghicov, P. Schmuki, Mechanistic aspects of the self-organization process for oxide nanotube formation on valve metals, J. Electrochem. Soc. 154 (2007) C472-C478.

[36] K. Lu, Z. Tian, J.A. Geldmeier, Polishing effect on anodic titania nanotube formation, Electrochim. Acta 56 (2011) 6014-620.

[37] H. Tsuchiya, S. Berger, J. M. Macak, A. Ghicov, P. Schmuki, Self-organized porous and tubular oxide layers on Ti Al alloys, Electrochem. Commun. 9 (2007) 2397-2402.

[38] S. Berger, H. Tsuchiya, P. Schmuki, Transition from nanopores to nanotubes: Self-ordered anodic oxide structures on titanium-aluminides, Chem. Mater. 20 (2008) 3245-3247.

[39] A. Dronov, I. Gavrilin, E. Kirilenko, D. Dronova, S. Gavrilov, Investigation of anodic TiO_2 nanotube composition with high spatial resolution AES and ToF SIMS, Appl. Surf. Sci. 434 (2018) 148-154.

[40] J. M. Macak, P. Schmuki, Anodic growth of self-organized anodic TiO_2 nanotubes in viscous electrolytes, Electrochim. Acta 52 (2006) 1258-1264.

[41] S. Albu, P. Schmuki, Influence of anodization parameters on the expansion factor of TiO_2 nanotubes, Electrochim. Acta 91 (2013) 90-95.

[42] G. Zhang, H Huang, Y. Zhang, Helen L.W. Chan, L. Zhou, Highly ordered nanoporous TiO_2 and its photocatalytic properties, Electrochem. Commun. 9 (2007) 2854-2858.